


CASQ1 mutations impair calsequestrin polymerization and cause tubular aggregate myopathy

Johann Böhm¹ · Xavière Lornage¹ · Frederic Chevessier² · Catherine Birck¹ · Simona Zanotti³ · Paola Cudia⁴ · Monica Bulla⁵ · Florence Granger¹ · Mai Thao Bui⁶ · Maxime Sartori¹ · Christiane Schneider-Gold⁷ · Edoardo Malfatti⁶ · Norma B. Romero⁶ · Marina Mora³ · Jocelyn Laporte¹ 

Received: 7 September 2017 / Revised: 10 October 2017 / Accepted: 10 October 2017
© Springer-Verlag GmbH Germany 2017

Tubular aggregate myopathy (TAM) is a rare muscle disorder characterized by abnormal accumulations of membrane tubules in muscle fibers, and marked by progressive muscle weakness, cramps, and myalgia [3]. Genetically, TAM has been assigned to mutations in *STIM1* [2] and *ORAI1* [7], both encoding key regulators of Ca²⁺ homeostasis. Through exome sequencing of molecularly undiagnosed TAM cases, we now identified *CASQ1* as the third TAM gene, and we support our findings by clinical, histological, genetic, and functional data.

Family 1 has an ancestral history of a muscle phenotype segregating as a dominant disease, and a partial clinical and histological description was reported earlier [8]. Patient 103901 from Family 2 is a singleton. Birth, early childhood, and motor milestones were normal for all affected members from both families. Disease onset was between early 20s and mid-40s with a slowly progressive muscle weakness mainly

involving the proximal muscles in the lower limbs for Family 1, and early 50s with post-exercise myalgia in the lower limbs for Family 2 (Supplementary Table 1). Histological and ultrastructural analyses of the muscle biopsies displayed tubular aggregates as the main histopathological hallmark in both families (Fig. 1a). Exome sequencing identified the heterozygous *CASQ1* missense mutations c.166A>T (N56Y) in exon 1 in Family 1, and c.308G>A (G103D) in exon 2 in Family 2. Both mutations affect highly conserved amino acids (Supp. Figure 1), none was found in the available healthy family members, and none was listed in the public or internal SNP databases. A single *CASQ1* missense mutation (D244G) has previously been associated with vacuolar myopathy involving protein aggregates [9]. *CASQ1* is primarily expressed in skeletal muscle and encodes calsequestrin, the major Ca²⁺ storage protein in the sarcoplasmic reticulum. Calsequestrin binds Ca²⁺ with moderate affinity and high capacity, and forms higher order polymers with increasing Ca²⁺-binding capacities [4].

Immunohistochemistry on a muscle biopsy from Family 2 revealed strong signals for calsequestrin, STIM1, and RyR1 in aggregated structures most likely corresponding to the tubular aggregates, while ORAI1 was not trapped (Fig. 1b). This conforms to the observations made on biopsies from *STIM1* and *ORAI1* patients and demonstrates that the trapped proteins are primarily of sarcoplasmic reticulum origin [1, 2]. These findings on a single muscle biopsy also suggest that aggregation of STIM1 appears to be a consequence of *CASQ1* mutations, providing a pathological link between *STIM1*- and *CASQ1*-related TAM. In transfected C2C12 myoblasts, WT and both TAM N56Y and G103D mutants formed calsequestrin networks of comparable complexity, while the vacuolar myopathy D244G mutant induced major calsequestrin aggregation (Fig. 1c). Calsequestrin polymerization and depolymerization are dynamic

Electronic supplementary material The online version of this article (doi:10.1007/s00401-017-1775-x) contains supplementary material, which is available to authorized users.

✉ Johann Böhm
johann@igbmc.fr

✉ Jocelyn Laporte
jocelyn@igbmc.fr

¹ IGBMC, Inserm U 964, CNRS UMR 7104, University of Strasbourg, Illkirch, France

² CureVac AG, Tübingen, Germany

³ IRCCS Istituto Neurologico C. Besta, Milan, Italy

⁴ IRCCS San Camillo Hospital, Venice, Italy

⁵ University of Geneva, Geneva, Switzerland

⁶ Institut de Myologie, Paris, France

⁷ Ruhr-University Bochum, Bochum, Germany

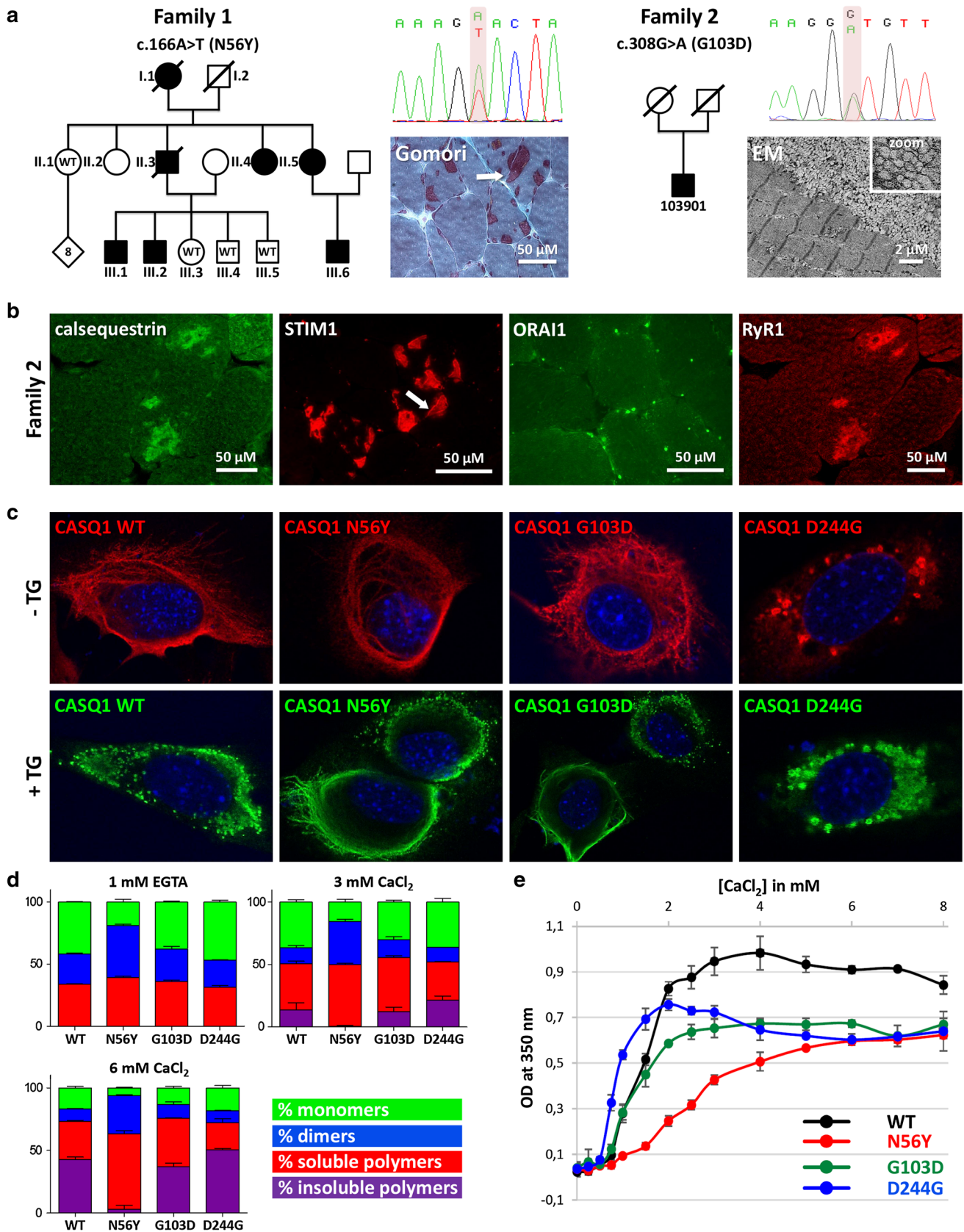


Fig. 1 Impact of the *CASQ1* mutations and immunohistochemistry on muscle biopsies. **a** Heterozygous *CASQ1* missense mutations segregating with the disease were identified in both families displaying tubular aggregates on muscle biopsies (arrow, zoom). **b** Immunohistochemistry on the biopsy from Family 2 revealed aggregation of calsequestrin, STIM1, and RyR1, but not of ORAI1. The STIM1 signals were thereby more pronounced in the periphery of the aggregated structures (arrow), while calsequestrin and RyR1 were also found in the center. **c** In Ca^{2+} -containing medium, WT calsequestrin and the N56Y and G103D mutants formed complex networks in transfected C2C12 myoblasts, while the D244G mutant aggregated. Ca^{2+} store depletion through addition of Thapsigargin (Tg) induced major monomerization of WT calsequestrin, while the N56Y and G103D mutants remained in large parts polymeric. **d** Analytical ultracentrifugation showed that especially the TAM N56Y mutant formed less insoluble higher order polymers at rising Ca^{2+} concentrations compared to the wild type, while the vacuolar myopathy D244G strongly polymerized. **e** Turbidity assays confirmed the reduced propensity of both TAM mutants to polymerize at rising Ca^{2+} concentrations

Ca^{2+} -dependent processes, and the depletion of the SR Ca^{2+} stores was shown to favor the monomeric form of calsequestrin [6]. To test whether the *CASQ1* mutations influence calsequestrin monomerization upon Ca^{2+} store depletion, we treated the transfected cells ($n > 300$ per condition) with the SERCA inhibitor Thapsigargin (Tg). Dot-like calsequestrin signals corresponding to monomers or minor oligomers were seen in the majority (76%) of the cells expressing the WT, but only in 49.4% and 42.5% of the cells, respectively, expressing N56Y or G103D. To investigate the impact of the *CASQ1* mutations on calsequestrin polymerization, we performed analytical ultracentrifugation in solution containing recombinant calsequestrin and rising Ca^{2+} concentrations (Fig. 1d). We found that especially the TAM N56Y mutant formed significantly less higher order polymers than the wild-type, while the vacuolar myopathy D244G mutant showed an increased propensity to form insoluble polymers. To follow the polymerization kinetics of WT and mutant calsequestrin, we next performed turbidity assays (Fig. 1e). G103D and especially N56Y calsequestrin show reduced polymerization rates, and produced significantly less polymers at maximal Ca^{2+} levels compared to the wild-type protein. Contrasting wild-type and TAM calsequestrin, the D244G mutant strongly polymerized at minimal Ca^{2+} levels, confirming the results obtained by a previous study [5].

Taken together, we demonstrate that specific *CASQ1* mutations are one of the genetic causes of TAM. We show that the tubular aggregates in our patients contain calsequestrin, STIM1, and RyR1, and we provide functional evidence that *CASQ1* mutations significantly impair calsequestrin polymerization and depolymerization, while the vacuolar myopathy mutation increases Ca^{2+} -dependent

polymerization. This suggests that the *CASQ1* mutations causing either TAM or vacuolar myopathy involve different pathomechanisms.

Acknowledgements We thank the members of the families for their interest in this study, Wolfram Kress, Michel Fardeau, and Daniel Hantai for material transfer, and Catherine Koch, Anaïs Chanut, and Raphaël Schneider for their valuable technical assistance. This work was funded by INSERM, CNRS, University of Strasbourg, Agence Nationale de la Recherche (ANR-11-BSV1-026, ANR-10-LABX-0030-INRT, ANR-10-IDEX-0002, and FRISBI ANR-10-INBS-05), Fondation Maladies Rares, Association Française contre les Myopathies (AFM-17088), the Muscular Dystrophy Association (MDA-186985), and the Swiss National Science Foundation (323530_158118 to MB). The EuroBioBank and Telethon Network of Genetic Biobanks (GTB12001F to MM) are gratefully acknowledged for providing biological samples.

References

- Bohm J, Bulla M, Urquhart JE, Malfatti E, Williams SG, O'Sullivan J, Szlauer A, Koch C, Baranello G, Mora M et al (2017) ORAI1 mutations with distinct channel gating defects in tubular aggregate myopathy. *Hum Mutat*. doi:10.1002/humu.23172
- Bohm J, Chevessier F, Maues De Paula A, Koch C, Attarian S, Feger C, Hantai D, Laforet P, Ghorab K, Vallat JM et al (2013) Constitutive activation of the calcium sensor STIM1 causes tubular-aggregate myopathy. *Am J Hum Genet* 92:271–278. doi:10.1016/j.ajhg.2012.12.007S0002-9297(12)00641-6
- Chevessier F, Bauche-Godard S, Leroy JP, Koenig J, Paturneau-Jouas M, Eymard B, Hantai D, Verdiere-Sahuque M (2005) The origin of tubular aggregates in human myopathies. *J Pathol* 207:313–323. doi:10.1002/path.1832
- Damiani E, Salvatori S, Margreth A (1990) Characterization of calsequestrin of avian skeletal muscle. *J Muscle Res Cell Motil* 11:48–55
- Lewis KM, Ronish LA, Rios E, Kang C (2015) Characterization of two human skeletal calsequestrin mutants implicated in malignant hyperthermia and vacuolar aggregate myopathy. *J Biol Chem* 290:28665–28674. doi:10.1074/jbc.M115.686261
- Manno C, Figueroa LC, Gillespie D, Fitts R, Kang C, Franzini-Armstrong C, Rios E (2017) Calsequestrin depolymerizes when calcium is depleted in the sarcoplasmic reticulum of working muscle. *Proc Natl Acad Sci USA* 114:E638–E647. doi:10.1073/pnas.1620265114
- Nesin V, Wiley G, Kousi M, Ong EC, Lehmann T, Nicholl DJ, Suri M, Shahrizaila N, Katsanis N, Gaffney PM et al (2014) Activating mutations in STIM1 and ORAI1 cause overlapping syndromes of tubular myopathy and congenital miosis. *Proc Natl Acad Sci USA* 111:4197–4202. doi:10.1073/pnas.1312520111
- Rohkamm R, Boxler K, Ricker K, Jerusalem F (1983) A dominantly inherited myopathy with excessive tubular aggregates. *Neurology* 33:331–336
- Rossi D, Vezzani B, Galli L, Paolini C, Toniolo L, Pierantozzi E, Spinozzi S, Barone V, Pegoraro E, Bello L et al (2014) A mutation in the *CASQ1* gene causes a vacuolar myopathy with accumulation of sarcoplasmic reticulum protein aggregates. *Hum Mutat* 35:1163–1170. doi:10.1002/humu.22631

1 **CASQ1 mutations impair calsequestrin polymerization and cause tubular**
 2 **aggregate myopathy**

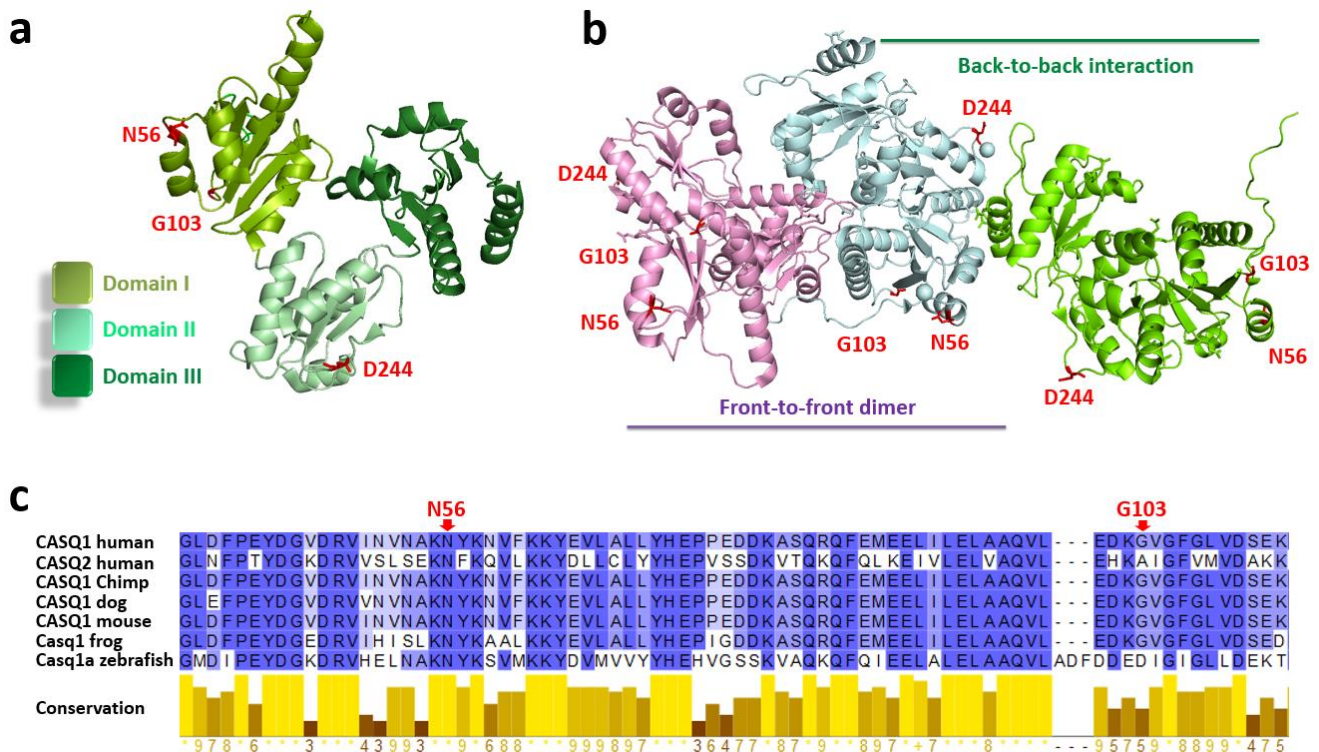
3 J Böhm, X Lornage, F Chevessier, C Birck, S Zanotti, P Cudia, M Bulla, F Granger, MT Bui,
 4 M Sartori, C Schneider-Gold, E Malfatti, NB Romero, M Mora, J Laporte

5 **Supplementary Material**

6 **FIGURES AND TABLES**

7 **Supp. Fig. 1 - Localization and conservation of the mutated calsequestrin residues**

8 (a) Position of the TAM (N56Y, G103D) and vacuolar myopathy (D244G) mutations on the
 9 resolved protein structure of a calsequestrin monomer. (b) None of the TAM mutations resides
 10 in the sites for front-to-front dimerization or back-to-back polymerization of calsequestrin. The
 11 vacuolar myopathy D244G mutation has been shown to impact on the back-to-back
 12 interactions of calsequestrin dimers [1] (c) All three mutations affect conserved amino acids of
 13 calsequestrin.



Supp. Table 1 - Genetic, clinical and histological features in TAM patients with *CASQ1* mutations

	Family 1							Family 2
Individual	I.1	II.3	II.4	II.5	III.1	III.2	III.6	103901
Gender	F	M	F	F	M	M	M	M
Mutation	c.166A>T p.Asn56Tyr	c.166A>T p.Asn56Tyr	c.166A>T p.Asn56Tyr	c.166A>T p.Asn56Tyr	c.166A>T p.Asn56Tyr	c.166A>T p.Asn56Tyr	c.166A>T p.Asn56Tyr	c.308G>A p.Gly103Asp
Onset	40s	40s	20s	20s	40s	20s	20s	50s
Age at last examination	no examination	59	73	68	50	32	42	58
Muscle symptoms	weakness of lower limbs	weakness of upper and lower limbs, shoulder girdle	weakness of lower limbs, anterior neck	weakness of lower limbs, anterior neck	weakness of upper and lower limbs, shoulder girdle, anterior neck, fatigability	weakness of upper and lower limbs, shoulder girdle	weakness of upper and lower limbs, shoulder girdle, anterior neck	post-exercise myalgia in lower limbs
Walking	difficulty climbing stairs	difficulty climbing stairs	difficulty climbing stairs	difficulty climbing stairs, frequent falls	difficulty climbing stairs, frequent falls	difficulty climbing stairs	normal	unable to walk on heels
CK level (U/L)	NA	normal	normal	normal	normal	normal	2 x	normal
Histology	NA	NA	TAs in type II fibers, fiber size variability, internalized nuclei	TAs in type II fibers, fiber size variability, internalized nuclei	TAs in type II fibers, fiber size variability, internalized nuclei	TAs in type II fibers, fiber size variability, internalized nuclei	TAs in type II fibers, fiber size variability, internalized nuclei	TAs in type II fibers, fiber size variability, internalized nuclei
Signs of Stormorken syndrome	NA	no	no	no	no	no	no	ichthyosis
Other features	NA	calf hypertrophy	three pregnancies with still birth	calf hypertrophy, one pregnancy with still birth	no	no	no	no

NA = not assessed

1 MATERIALS AND METHODS

2 Patients

3 Informed consent was obtained from all individual participants included in the study, and DNA
4 collection and experimentation were performed following institutional IRB-accepted protocols
5 and the Comité de Protection des Personnes Est IV (DC-2012-1693), and according to the
6 declaration of Helsinki. Patients were from Germany (Family 1), and Italy (Family 2).

7 Sequencing and segregation analysis

8 Exome sequencing was carried out for patients II.4, III.1, III.6, as well as for the unaffected
9 individual II.1 from Family 1. Targeted sequences were captured using the Agilent SureSelect
10 Human all Exon Kit (Santa Clara, USA), and enriched DNA fragments were sequenced on an
11 Illumina Genome Analyzer Iix (San Diego, USA) to generate 72nt single reads. Sequence data
12 were aligned to the GRCh37/hg19 reference genome using the Burrows-Wheeler aligner
13 software (<http://bio-bwa.sourceforge.net>), and variant calling was performed with SAMtools
14 [3]. Following databases were used for SNP annotation and filtering: Exome Variant Server
15 (<http://evs.gs.washington.edu/EVS/>), ExAC (<http://exac.broadinstitute.org/>), and dbSNP
16 (<http://www.ncbi.nlm.nih.gov/projects/SNP/>), as well as our in-house exome database
17 containing 1662 exomes including 650 control exomes. Impacts of variations were predicted
18 using Alamut v.2.5 (<http://www.interactive-biosoftware.com>) and VaRank [1].

19 For patient 103901 from Family 2, direct Sanger-sequenced for the *CASQ1* coding exons and
20 the adjacent splice-relevant regions was performed. Segregation analyses for Family 1 was also
21 performed by Sanger sequencing. The *CASQ1* mutations were numbered according to
22 GenBank NM_001231.4 and NP_001222.3. Nucleotide position reflects cDNA numbering

1 with +1 corresponding to the A of the ATG translation initiation codon. All identified mutations
2 have been submitted to the LOVD database (<http://www.lovd.nl/CASQ1>).

3 **Histology and electron microscopy**

4 For histology, transverse sections (10 μ m) of the muscle biopsies were stained with modified
5 Gomori Trichrome and assessed for fiber morphology and accumulations/infiltrations.

6 For electron microscopy, muscle sections were fixed in 2.5% paraformaldehyde, 2.5%
7 glutaraldehyde, and 50 mM CaCl₂ in 0.1 M cacodylate buffer (pH 7.4). Samples were postfixed
8 with 2% OsO₄, 0.8% K₃Fe(CN)₆ in 0.1 M cacodylate buffer (pH 7.4) for 2 h at 4°C and
9 incubated with 5% uranyl acetate for 2 h at 4°C. Muscles were dehydrated in a graded series
10 of ethanol and embedded in epon resin. Thin sections were examined with an electron
11 microscope (Philips CM120 or 410, FEI Company, Hillsboro, USA).

12 **Protein studies**

13 Immunofluorescence was performed with routine protocols using following antibodies: mouse
14 anti-calsequestrin (Affinity BioReagents, Golden, USA), mouse anti-GOK/Stim1 (BD
15 Biosciences, Franklin Lakes, USA), rabbit anti-Orai1 (Abcam, Paris, France), mouse anti-
16 Ryanodine receptor (Affinity BioReagents), and appropriate Alexa Fluor secondary antibodies
17 (Invitrogen, Carlsbad, USA). Nuclei were stained with Hoechst (Sigma-Aldrich). Sections
18 were mounted with antifade reagent (Invitrogen) and viewed using a laser scanning confocal
19 microscope (TCS SP2, Leica Microsystems, Wetzlar, Germany).

20 **Constructs**

21 CASQ1 expression constructs were generated by PCR amplification of skeletal muscle cDNA
22 from a healthy individual. PCR fragments containing the complete ORF were cloned into the
23 pCS2 vector without tag (Addgene, Cambridge, USA) for the localization experiments, the

1 pAAV-IRES-hrGFP vector (Cell Biolabs, San Diego, USA) for the Ca²⁺ experiments, and the
2 pGEX6-P-1 vector containing an N-terminal GST tag followed by a PreScission protease site
3 (GE Healthcare, Little Chalfont, UK) for the production of recombinant proteins. The CASQ1-
4 pGEX6-P-1 construct used for the turbidity assay lacks the most 5' nucleotides coding for the
5 ER localization signal (amino acids 1-34). The *CASQ1* point mutations (c.166A>T, c.308G>A,
6 c.731A>G) were introduced by site-directed mutagenesis using the *Pfu* DNA polymerase
7 (Stratagene, La Jolla, USA).

8 **Cells and transfections**

9 C2C12 murine myoblasts were cultured in DMEM supplemented with 10% fetal bovine serum
10 (10270-106), 5 µg/ml streptomycin and 5 units/ml penicillin (all Gibco Life Technologies
11 Carlsbad, USA), and maintained at 37°C in 5% CO₂. Cells were transfected at 50% confluency
12 with Lipofectamine® 2000 (Invitrogen), fixed with 4% PFA in PBS for 24 h, mounted on
13 slides, and analyzed by fluorescence microscopy. Passive Ca²⁺ store depletion was induced by
14 the addition of 1 µM Thapsigargin (Sigma-Aldrich). The localization experiments were
15 repeated three times.

16 **Purification of calsequestrin**

17 Proteins were expressed in *E. coli* BL21 in LB media by IPTG-induction for 18 h at 20°C.
18 Bacteria were lysed by sonication in buffer containing 30 mM Tris pH 7.5, 500 mM NaCl,
19 1 mM EDTA, 0.5 mM DTT, and supplemented with EDTA-free complete protease inhibitor
20 cocktail (Roche, Basel, Switzerland) and DNase (Expedeon, Swavesey, UK). GST-tagged
21 proteins were purified by affinity chromatography using Glutathione sepharose in batch mode.
22 The cleaved proteins were eluted after overnight incubation at 4°C with PreScission protease
23 loaded on anion exchange chromatography (Bio-Rad, Hercules, USA), and further eluted in a
24 50 - 1000 mM NaCl gradient. Proteins were concentrated to 8 mg/ml using Amicon-Ultra filter

1 units and stored in 20 mM Tris pH 7.5, 300 mM NaCl, and 1 mM EGTA at -80°C after flash
2 freezing in liquid nitrogen.

3 **Analytical ultracentrifugation**

4 Sedimentation velocity experiments were performed in a Beckman-Coulter XL-I analytical
5 ultracentrifuge (Brea, USA) at 4°C and 50 000 rpm. Wild type and mutant recombinant
6 calsequestrin were prepared at 13 µM in 20 mM Tris pH 7.5, 300 mM NaCl, 1 mM EGTA plus
7 0, 3, or 6 mM CaCl₂, and absorbance scans were taken at 280 nm every 6 minutes. The
8 sedimentation data were analyzed with the Sedfit program [4] using the sedimentation
9 coefficient distribution model. The integration of the peaks corresponding to monomers,
10 dimers and oligomers in the c(s) distributions gave the percentage of each species reported in
11 the histograms. Buffer density, buffer viscosity and protein partial specific volume were
12 calculated using the SEDNTERP software. Experiments were repeated three times, and the
13 statistical significance was determined by the Kruskal-Wallis test and the Dunn's multiple
14 comparison test.

15 **Turbidity assay**

16 Aggregation of human calsequestrin was measured as a function of Ca²⁺ concentration by
17 adding 1 µl of CaCl₂ stock solutions (0, 2.5, 5.0, 7.5, 10, 15, 20, 25, 30, 40, 50, 60, 70, 80 mM)
18 to 9 µl calsequestrin (2.8 µM) in 20 mM Tris pH 7.5, and 24 mM NaCl. After CaCl₂ addition,
19 protein samples were incubated to equilibrate for at least 5 min, and the absorbance was
20 recorded at 350 nm using a Nanodrop One spectrophotometer (Wilmington, USA). Absorbance
21 of samples was corrected by subtracting the absorbance of buffer alone. All turbidity
22 measurements were repeated three times. Statistical significance was assessed by the Kruskal-
23 Wallis test and the Dunn's multiple comparison test after calculation of the area under the
24 curves.

1 **REFERENCES**

- 2 1 Geoffroy V, Pizot C, Redin C, Piton A, Vasli N, Stoetzel C, Blavier A, Laporte J, Muller
3 J (2015) VaRank: a simple and powerful tool for ranking genetic variants. PeerJ 3: e796
4 Doi 10.7717/peerj.796
- 5 2 Lewis KM, Ronish LA, Rios E, Kang C (2015) Characterization of two human skeletal
6 calsequestrin mutants implicated in malignant hyperthermia and vacuolar aggregate
7 myopathy. J Biol Chem 290: 28665-28674 Doi 10.1074/jbc.M115.686261
- 8 3 Li H, Handsaker B, Wysoker A, Fennell T, Ruan J, Homer N, Marth G, Abecasis G,
9 Durbin R (2009) The sequence alignment/map format and SAMtools. Bioinformatics
10 25: 2078-2079 Doi btp352 [pii]10.1093/bioinformatics/btp352
- 11 4 Schuck P (2000) Size-distribution analysis of macromolecules by sedimentation
12 velocity ultracentrifugation and lamm equation modeling. Biophys J 78: 1606-1619 Doi
13 10.1016/S0006-3495(00)76713-0